Journal of Industrial and Engineering Chemistry 78 (2019) 84–89

Contents lists available at ScienceDirect

Journal of Industrial and Engineering Chemistry

journal homepage: www.elsevier.com/locate/jiec

Fabrication and thermal behavior of Al/Fe_2O_3 energetic composites for effective interfacial bonding between dissimilar metallic substrates

Ji Hoon Kim[a], Myung Hoon Cho[a], Hong-Min Shim[b], Soo Hyung Kim[a,c,*]

[a] Research Center for Energy Convergence Technology, Pusan National University, 2, Busandaehak-ro 63beon-gil, Geumjeong-gu, Busan 46241, Republic of Korea
[b] Agency for Defense Development, P.O. Box 35, Yuseong, Daejeon, 34186, Republic of Korea
[c] Department of Nanoenergy Engineering, College of Nanoscience and Nanotechnology, Pusan National University, 2, Busandaehak-ro 63beon-gil, Geumjeong-gu, Busan 46241, Republic of Korea

ARTICLE INFO

Article history:
Received 30 April 2019
Received in revised form 16 June 2019
Accepted 23 June 2019
Available online 28 June 2019

Keywords:
Energetic material
Solder material
Dissimilar substrates
Interfacial bonding
Aluminothermic reaction

ABSTRACT

Herein, the roles of an Al/Fe_2O_3 energetic composites as a heat energy source and a bonding medium for interfacially bonding dissimilar Al/Cu metallic substrates are systematically investigated. Energetic material (EM)/solder material (SM) bilayer pellets are assembled and ignited between the interfacial Al/Cu substrates for bonding. The upper EM layer comprising an Al microparticle (MP)/Al nanoparticle (NP)/Fe_2O_3 NP composite serves as a heat source for melting the lower SM layer comprising SAC305 MP for strongly bonding the Cu substrate with the melted SM layer. The intermetallic compounds (Al_xFe_y) formed during the aluminothermic reactions of the ignited EM layer play an important role as a bonding medium between the Al substrate and the melted EM layer. The dissimilar Al/Cu substrates are interfacially bonded using an EM layer with a fuel-to-oxidizer ratio of 1.97–4.44. The maximum mechanical strength of the bonded Al/Cu substrates increases with the increase in the fuel-to-oxidizer ratio owing to the supply of sufficient heat energy under fuel-rich conditions. The EM layer acts as an effective heat energy source and mechanical bonding medium. The proposed interfacial bonding technique is simple, easy, and versatile for welding and joining dissimilar metallic substrates for industrial applications.

Introduction

Metal substrates can be bonded using various welding methods. In the conventional liquid-state welding method, which is also called fusion welding, a joint is formed by melting the base metals through chemical or electric means using electric resistance, gas, laser, and thermites [1]. This method is mainly used for bonding substrates made of the same metal. Recently, the demand for bonding dissimilar metals, such as Al–steel [2,3], Al–Mg [4–6], and Al–Cu [7–15], has been growing in many fields, including aeronautical, automotive, and electronics industries, for weight reduction, enhanced thermal and electrical properties, and cost reduction. However, it is difficult to apply the conventional liquid-state welding method for bonding dissimilar metals because of the differences in their physical and chemical properties such as the melting point and thermal expansion coefficient [7,8,13,16].

To overcome these problems, solid/liquid- or solid-state welding methods have been used to bond dissimilar metals. In solid/liquid-state welding methods (e.g., soldering and brazing), filler materials having melting points lower than those of the base metals are used to make a joint. The selection of the filler materials is an important factor for a successful bonding, because the physical properties of the filler materials (e.g., wettability and melting point) should be compromised with dissimilar metals. Thus, numerous studies have been conducted on developing versatile filler materials suitable for bonding various dissimilar metals [7,10,12]. Solid-state welding techniques (e.g., friction stir welding [8,9,13,16] and explosive welding [11]) have been rapidly developed for bonding dissimilar metals in recent years. In this method, fusion deformation rarely occurs in the heated area, thus ensuring high-quality joints. However, the relatively long welding cycle is a major disadvantage, limiting its widespread practical applications [14]. Several previous studies for relatively rapid bonding process with reactive multilayer foils have been also

* Corresponding author at: Department of Nanoenergy Engineering, College of Nanoscience and Nanotechnology, Pusan National University, 2, Busandaehak-ro 63beon-gil, Geumjeong-gu, Busan 46241, Republic of Korea.
E-mail address: sookim@pusan.ac.kr (S.H. Kim).

https://doi.org/10.1016/j.jiec.2019.06.041
1226-086X/

reported. The reactive multilayer foils were successfully used as a rapid heat generation source to melt neighboring solder materials for bonding dissimilar metals. However, the fabrication of reactive multilayer foil has the disadvantage of requiring very sophisticated manufacturing processes (e.g., sputtering [17,18], mechanical swaging and rolling [19]).

In this study, we propose a simple, easy, and versatile bonding technique using an energetic material (EM) as both heat generating source and bonding medium to overcome the limitations of the conventional liquid- and solid/liquid-state welding techniques. An EM is a composite made of a metal and an oxidizer, which undergo a redox reaction when ignited, thus rapidly emitting thermal energy [20–23]. We focused on the direct bonding between an Al substrate and an EM via fusion and atomic diffusion. The major advantage of employing an EM is that various metal fuels (e.g., Al [20–34], Mg [31,33], and Si [24,35,36]) and oxidizers (e.g., CuO [21,22,27,29,32], NiO [26,30], Fe_2O_3 [23,28], MoO_3 [25,32,34], and WO_3 [32]) can be used as components for the interfacial bonding of dissimilar metals. We strongly believe that an EM with various components can be potentially employed to join dissimilar metals and help improve the resulting mechanical strength of the bonded metals [2,3,7–10,12,15]. In this study, the composition and combustion characteristics of an EM used for the interfacial bonding of dissimilar Al/Cu metallic substrates are investigated. The combustion characteristics of the EM (such as the total exothermic heat, burn rate, and total burning time) are controlled by systematically changing the chemical compositions of the EM. Finally, the microstructures and mechanical bonding strength of the bonded Al/Cu substrates are analyzed using various techniques including SEM, EDS, and tensile strength testing.

Experimental

A mixture of Al nanoparticles (Al NPs; Nano Technology Co., Ltd., Korea) with an average diameter of ~80 nm and Al microparticles (Al MPs; Metal Player Co., Ltd., Korea) with an average diameter of ~8 μm was used as the fuel source. Fe_2O_3 NPs (Sigma-Aldrich, Korea) with an average diameter of ~90 nm was used as the oxidizer. SAC 305 powder (Sn: 96.5 wt%, Ag: 3.0 wt%, Cu: 0.5 wt%; Senju Metal Industry Co., Ltd., Japan) with an average diameter of

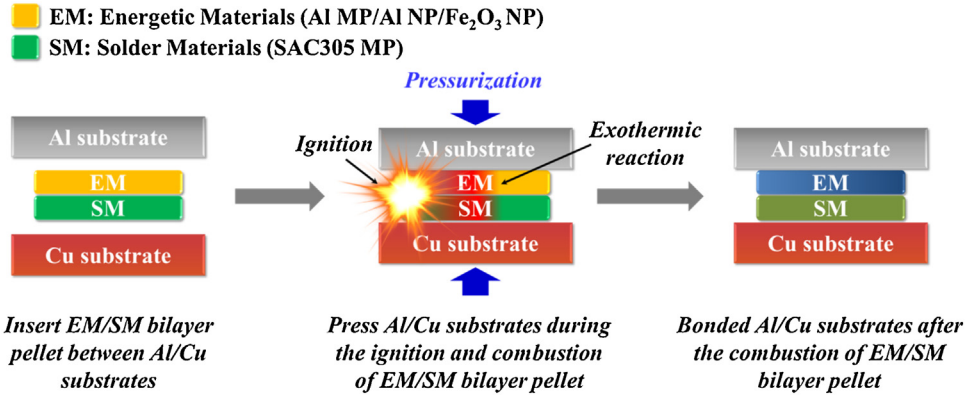

Fig. 1. Schematic of an interfacial bonding process for dissimilar Al/Cu substrates using an EM/SM bilayer pellet fabricated by die-compaction process.

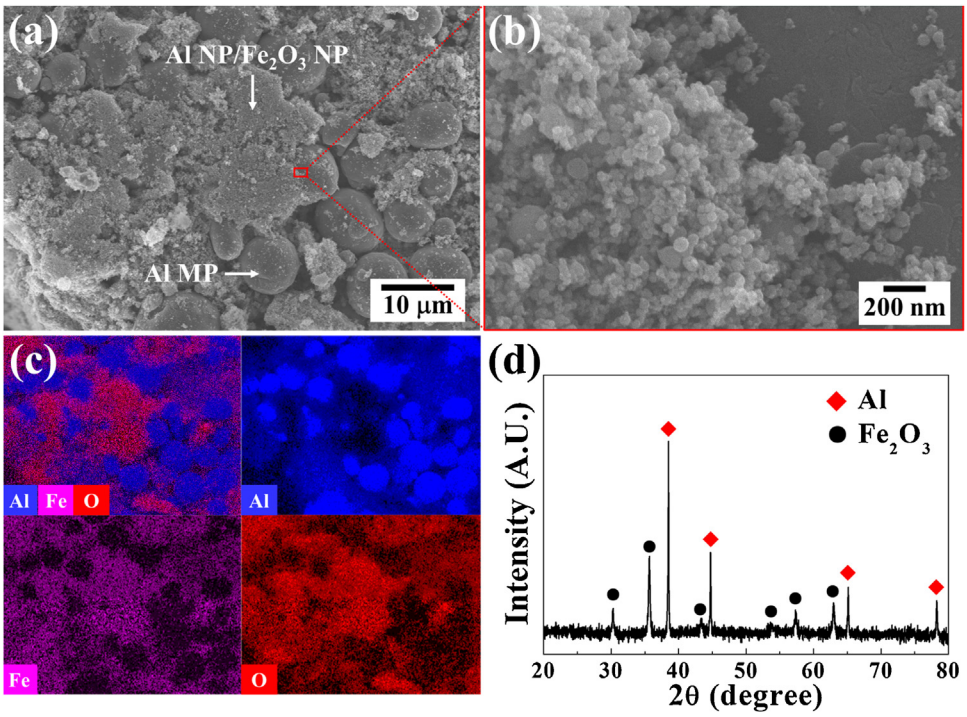

Fig. 2. (a) LR-SEM image, (b) HR-SEM image, (c) EDS image (elemental map), and (d) XRD results of Al NP/Al MP/Fe_2O_3 NP composite-based EM powder.

~70 μm was used as the solder material (SM). EM powders composed of Al NPs/Al MPs/Fe_2O_3 NPs were dispersed in an ethanol solution using an ultrasonication process (ultrasonic power: 170 W, ultrasonic frequency: 40 kHz) for 30 min and subsequently dried in a convection oven at 80 °C for 30 min. Finally, the EM (i.e., Al NP/Al MP/Fe_2O_3 NP composite) and SM (i.e., SAC305 MP) powders were sequentially poured into a mold in a die-compaction process and then pelletized into a disk (diameter: 10 mm, height: ~1 mm) under a pressure of 300 MPa. Fig. 1 shows a schematic of the interfacial bonding process for dissimilar Al/Cu substrates using the EM/SM bilayer pellet, which was formed via the die-compaction process. The fabricated EM/SM bilayer pellet was inserted between the Al/Cu substrates, and the interfacial bonding process was then implemented by igniting the bilayer pellet using a hot-wire at an applied voltage of 4 V and a current of 2 A. It should be noted that the addition of highly reactive Al NPs as a fuel source in the EM layer was intended to stably ignite the composite pellet with lower heat energy input and simultaneously promote the combustion process of Al MPs in the EM layer. However, we observed that the use of Al NPs without adding Al MPs in the EM layer resulted in highly active combustion reaction when ignited and thus the resulting EM layer was exploded so that the stable bonding process for dissimilar substrates was not successful.

The physical structures and elemental maps of the EM powder and Al/Cu substrates with the EM/SM composite pellet before and after the bonding process were observed using a field emission scanning electron microscope (FE-SEM, Carl Zeiss, Supra 25, Germany) operated at ~20 kV and equipped with an energy dispersive X-ray analyzer (EDS, Oxford Instruments, INCA, UK). An X-ray diffraction analyses of the EM powder and the interface between Al substrate and EM pellet after bonding were performed using an X-ray diffractometer (XRD, PANalytical, X'Pert^3 Powder, Netherlands) with Cu Kα radiation in the range of 10–90°. Differential scanning calorimetry (DSC; Setaram, LABSYS evo, France) measurements of the EM powders were performed at a heating rate of 10 °C min^{-1} in a temperature range of 30–1000 °C under Ar atmosphere. A high-speed camera (Photron, FASTCAM SA3 120K, Japan) was employed to observe the ignition and combustion of the EM powders and pellets. After performing the interfacial bonding process, we measured the mechanical strength of the bonded Al/Cu substrates using a universal tensile strength tester (LRX Plus 5 kN, Lloyd Instruments Ltd., UK) at a strain rate of 10 mm min^{-1}.

Results and discussion

To examine the physical structures and chemical compositions of the EM powder composed of Al NP/Al MP/Fe_2O_3 NP fabricated in this study, SEM, EDS, and XRD analyses were performed. Fig. 2 shows the analysis results. The Al NPs and Al MPs (used as the fuel) are both spherical with average diameters of ~80 nm and ~8 μm,

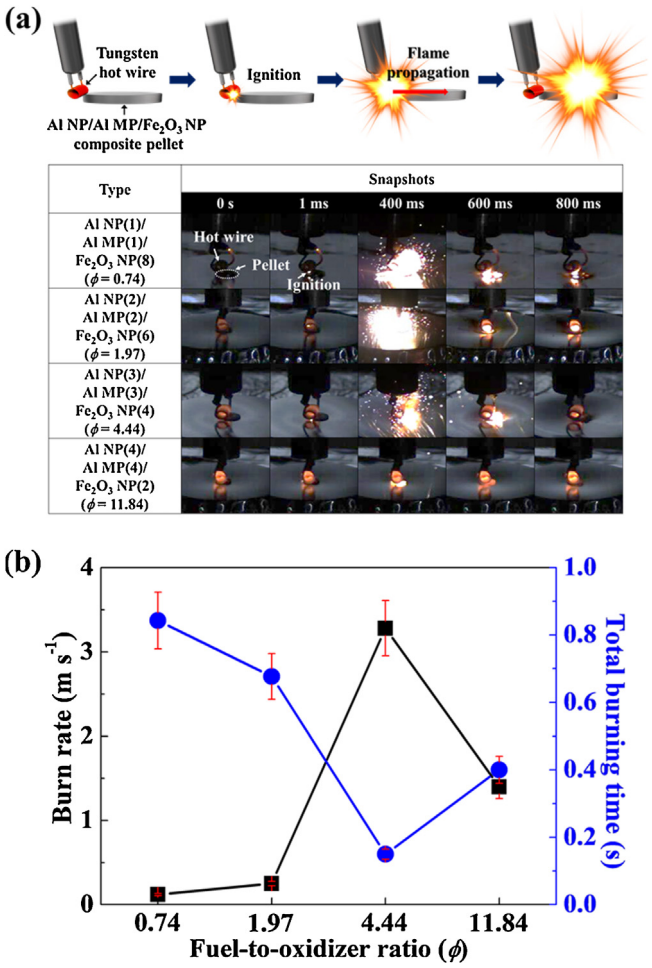

Fig. 3. (a) Schematic and snapshots of ignition and combustion tests and (b) resulting burn rate and total burning time of the Al NP/Al MP/Fe_2O_3 NP-based composite pellets with different fuel-to-oxidizer ratios.

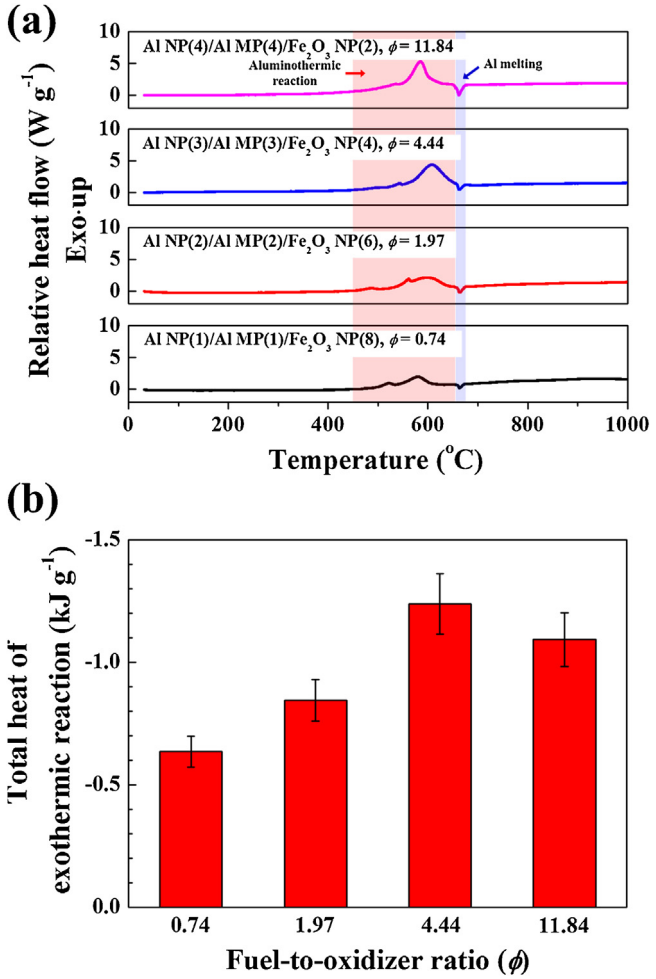

Fig. 4. (a) Differential scanning calorimetry (DSC) results, and (b) total heat energy generated from the exothermic and oxidation reactions of Al MP/Al NP/Fe_2O_3 NP-based composite pellet with various fuel-to-oxidizer ratios.

respectively (Fig. 2**a** and **b**). The Fe_2O_3 NPs (used as the oxidizer) are also spherical with an average diameter of 90 nm. After preparing the EM powder, Al NPs/Fe_2O_3 NPs were found to be homogeneously distributed and attached onto the surfaces of the Al MPs. This can be corroborated by the elemental mapping results shown in Fig. 2**c**. In addition, strong signals originating from both Al and Fe_2O_3 are observed for the EM powder in the XRD data, as shown in Fig. 2**d**.

The effects of the fuel-to-oxidizer ratio (ϕ) on the combustion characteristics of the Al NP/Al MP/Fe_2O_3 NP composite were examined. The fuel-to-oxidizer ratio of the composite pellets was determined using Eq. (1).

$$\phi = \frac{(Fuel/Oxidizer)_{Actual}}{(Fuel/Oxidizer)_{Stoichiometric}} \quad (1)$$

Various composite pellets made of Al MP (10–40 wt%)/Al NP (10–40 wt%)/Fe_2O_3 NP (20–80 wt%) were fabricated and then ignited using a hot-wire, as shown in Fig. 3**a**. After the initial ignition of the composite pellets, the flame propagation was monitored using a high-speed camera. The snapshots (Fig. 3**a**) show the combustion characteristics of the composite pellets with different fuel-to-oxidizer mixing ratios. The composite pellets were successfully ignited, and the generated flame propagated through the pellets. The burn rate was calculated by dividing the pellet diameter with the total time required for the flame to propagate from one end to the other end. The total burning time was determined as the time elapsed from the start of ignition at one end of the pellet to the reaching of the flame at the other end of the pellet. Fig. 3**b** shows the resulting burn rate and the total burning time of the composite pellets determined by analyzing the series of snapshots. The burn rate is significantly higher under fuel-rich conditions ($\phi > 1$) than under fuel-lean condition ($\phi < 1$). The thermal conductivity of the EM under fuel-rich conditions was enhanced owing to the abundance of Al fuel in the pellet [34,37,38]. Thus, the burn rate increased sharply with the increase in the fuel-to-oxidizer ratio, and the maximum burn rate was

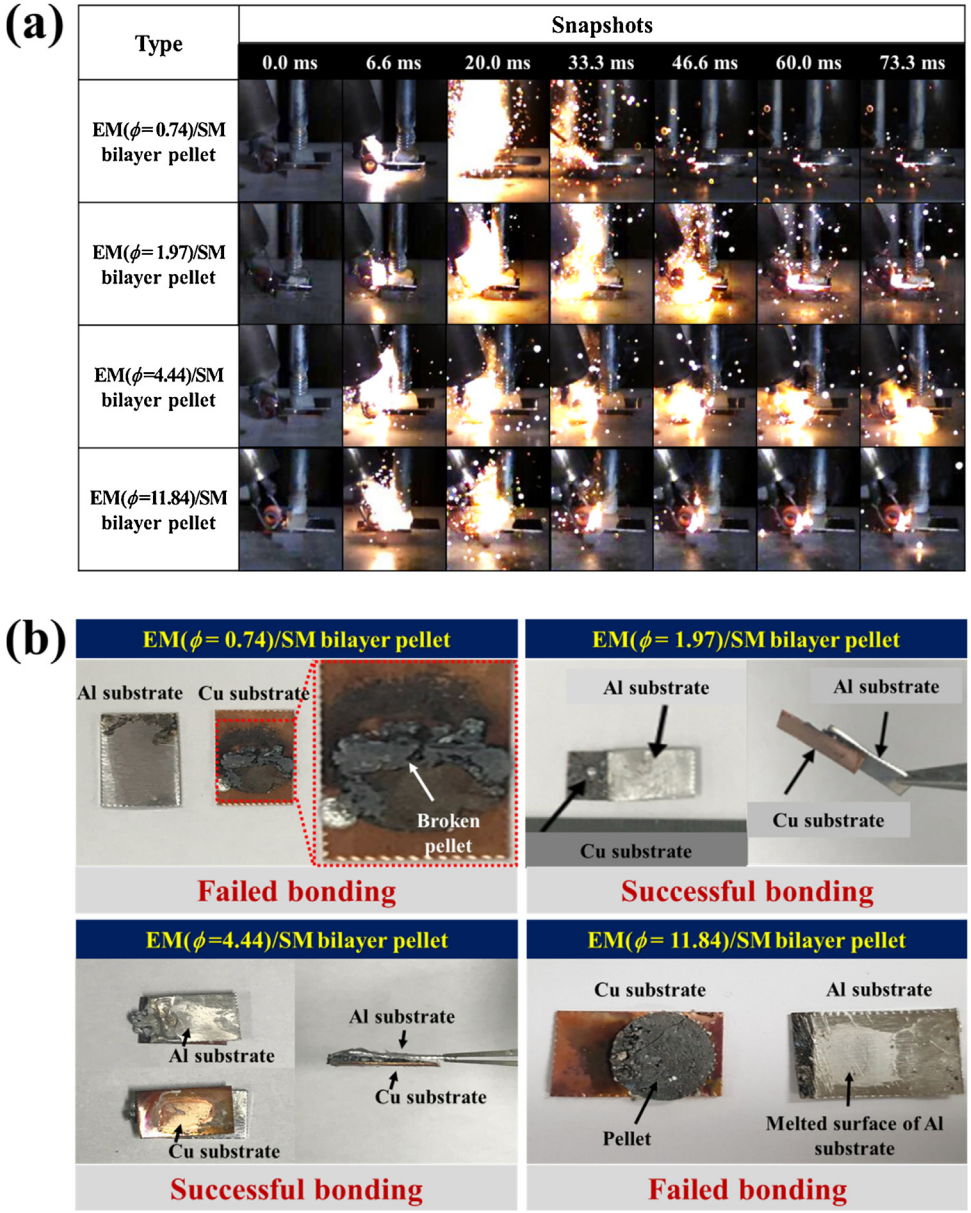

Fig. 5. (a) Snapshots of initial ignition and subsequent combustion process of EM/SM bilayer pellets with various fuel-to-oxidizer ratios for an interfacial bonding between Al and Cu substrates, and (b) images of top- and side-view of Al and Cu substrates after the combustion process of the EM/SM bilayer pellets.

found to be ~3.25 m s^{-1} when $\phi = 4.44$. However, it significantly decreased under excessive fuel-rich conditions ($\phi > 4.44$) because of the lack of oxidizer (i.e., Fe_2O_3 NPs), which rapidly provides oxygen to the fuel in the pellet. This suggests that the fuel-to-oxidizer ratio strongly affects the combustion characteristics of the Al NP/Al MP/Fe_2O_3 NP-based composite pellets. Thus, it is important to carefully select the fuel-to-oxidizer ratio for various thermal applications.

To examine the heat energy generated by the composite pellets with various fuel-to-oxidizer ratios, DSC analyses were performed. Fig. 4**a** shows the results. The first exothermic peak occurred by an aluminothermic reaction (i.e., $2Al + Fe_2O_3 \rightarrow Al_2O_3 + 2Fe + Heat$) and Al oxidation by ambient air in a temperature range of 500–600 °C. The secondary peak was appeared as an endothermic reaction at approximately 660 °C because the unreacted Al was melted. Fig. 4**b** summarizes the evolution of the total thermal energy generated during the exothermic reactions for composite pellets with a fuel-to-oxidizer ratio ranging from 0.74 to 11.84. The generated total heat energy was found to increase with increasing the amount of Al ($\phi = 0.74$–4.44), but it then decreased with the addition of further Al ($\phi > 4.44$). This suggests that the optimized Fe_2O_3 NP content in the Al MP/Al NP matrix was ~40 wt%, which was found to maximize the aluminothermic reaction of Al. The total exothermic heat energy range of 0.64–1.24 kJ g^{-1} measured in this study was very similar with other research results on Al/Fe_2O_3 nanocomposites (i.e., 0.33–1.03 kJ g^{-1}) [28]. However, the experimentally determined values for the total exothermic heat energy (≤1.5 kJ g^{-1}) were much lower than the theoretical value of ~3.9 kJ g^{-1}. We believe that this shortfall occurred due to an oxide layer forming on the surfaces of the Al particles and the incomplete oxidation of the Al in the fuel-rich conditions.

To test the interfacial bonding of the dissimilar Al/Cu materials, the EM/SM bilayer pellet fabricated in this study was installed between Al/Cu substrates with an area of 10 mm × 18 mm. Both sides of the Al/Cu substrates were covered using silicone rubber to prevent heat loss. Fig. 5**a** shows the initial ignition and combustion process of the EM/SM bilayer pellets inserted between the Al/Cu substrates. The initiated flame stably propagates through the EM/SM bilayer pellets with fuel-to-oxidizer ratios of 1.97 and 4.44, ultimately resulting in a successful interfacial bonding between the Al/Cu substrates (Fig. 5b). This suggests that the upper EM layer played an important role as a heat energy source as well as a bonding material between the Al substrate and the EM layer by forming an intermetallic compound; this can be corroborated by the EDS analysis results (see Fig. 6). However, it is interesting to note that the flame propagation is not stable for EM/SM bilayer pellets with fuel-to-oxidizer ratios of 0.74 and 11.84, in which case the Al and Cu substrates could not be bonded (Fig. 5b). This suggests that excessive fuel-lean and fuel-rich conditions result in adverse effects on the stable combustion of the EM/SM bilayer pellets.

Fig. 6 shows a cross-sectional SEM image and elemental maps of the Al and Cu substrates before and after the combustion process of the EM/SM bilayer pellets. The as-prepared EM/SM bilayer pellet uniformly contacts the Al and Cu substrates, respectively, (see Fig. 6a, **b** and **c**) before the combustion reaction of the pellet. However, after the combustion reaction of the upper EM layer, several bonded Al spots and a thin layer of intermetallic compounds are formed (See Fig. 6**d** and **e**) because of the reaction between the molten Al substrate and the reduced Fe. With the assistance of XRD analysis, strong peaks for Al/Al_2O_3/Fe and relatively weak peaks for intermetallic compounds of $AlFe_3$/$AlFe_4$ were found as shown in Fig. 6**f**. This suggests that the strong joint between the Al substrate and the upper EM layer was made by the formation of bonded Al spots and the partial support of intermetallic compounds. Moreover, the lower SM layer strongly attached onto the surface of the Cu substrate. The thermal diffusion of Sn and Cu was due to the relatively high-temperature environment during the combustion reaction of the EM layer. This finally resulted in a strong interfacial bonding between the Al/Cu substrates.

After the interfacial bonding process, a universal tensile strength test was performed on the interfacially bonded Al/Cu substrates to examine the mechanical bonding strength between the Al/Cu substrates, as shown in Fig. 7. The maximum tensile stresses of Al/Cu substrates bonded using EM/SM bilayer pellets with fuel-to-oxidizer ratios of 1.97 and 4.44 were found to be ~13.57 and ~15.63 MPa, respectively. The maximum mechanical strength of the Al/Cu substrate bonded using an EM/SM bilayer pellet with a higher fuel-to-oxidizer ratio (i.e., $\phi = 4.44$) increased by ~15% compared to when using an EM/SM bilayer pellet with $\phi = 1.97$. This was presumably because the exothermic energy was sufficient to strongly bond the pellet onto the substrates. The images of the fractured substrates (provided as insets) confirm that the Al substrate was torn to some extent by the upper EM layer of the pellet because of the strong mechanical joint. However, when the pellet was made with a lower fuel-to-oxidizer ratio (i.e., $\phi = 1.97$), the Al/Cu substrates detached because of the broken pellet. This is because the heat energy was not sufficient for this pellet to strongly bond the Al/Cu substrates. This shows that by controlling the fuel-to-oxidizer ratio of the EM/SM bilayer pellets, we can obtain an excellent mechanical bonding strength between dissimilar metallic substrates.

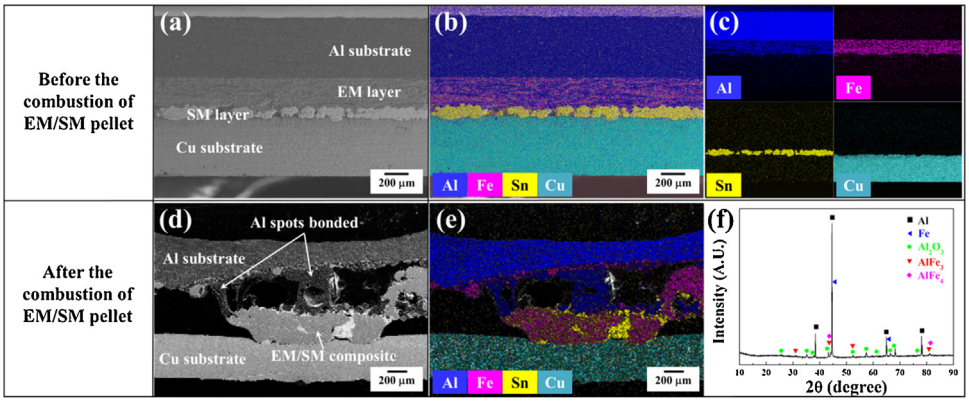

Fig. 6. (a, d) Cross-sectional SEM images and (b, d, e) EDS images of an EM/SM bilayer pellet inserted between Al/Cu substrates before and after the combustion process of the EM/SM bilayer pellet. (f) XRD diffraction pattern for the resulting materials formed between Al substrate and upper EM layer after interfacial bonding process. The upper EM layer in this sample comprises Al MP(2)/Al NP(2)/Fe_2O_3(6) with a fuel-to-oxidizer ratio of 1.97.

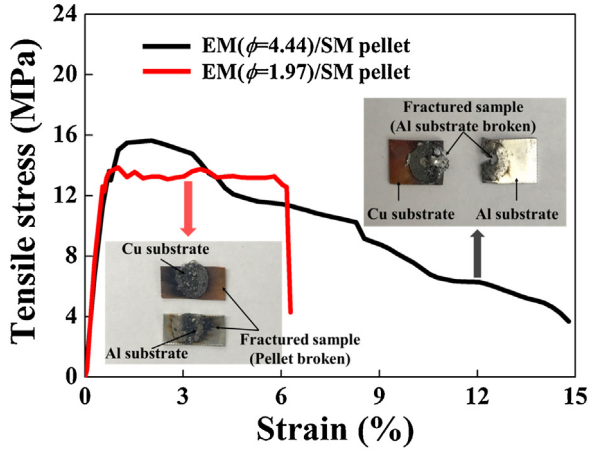

Fig. 7. Stress–strain curves for Al/Cu substrates bonded using EM/SM pellets with fuel-to-oxidizer ratios of 1.97 and 4.44.

Conclusions

In this study, we examined the effects of an EM as a heat energy source on melting the SM layer and as a bonding medium on forming intermetallic compounds in the interfacial bonding of dissimilar metallic substrates. The EM layer comprised Al MPs, Al NPs, and Fe_2O_3 NPs, respectively. The burn rate and exothermic energy of the EM layer increased with the increase in the fuel-to-oxidizer ratio. However, they significantly decreased under excessive fuel-rich conditions (i.e., $\phi > 4.44$) because of the lack of oxidizer. Finally, dissimilar Al/Cu substrates were interfacially bonded using EM/SM bilayer pellets. The resulting mechanical bonding strength of the bonded Al/Cu substrates increased with the increase in the fuel-to-oxidizer ratio in the EM layer. This suggests that the EM layer plays a key role as an effective heat energy source for melting the SM layer and as a bonding medium for forming intermetallic compounds. The proposed interfacial bonding process for dissimilar metallic substrates can be easily employed in various industrial welding and bonding applications.

Acknowledgments

This research was supported by the Civil & Military Technology Cooperation Program and Creative Materials Discovery Program through the National Research Foundation of Korea (NRF), funded by the Ministry of Science and ICT (No. 2013M3C1A9055407 & 2017M3D1A1039287). This research was also partially supported by the Agency for Defense Development funded by the Defense Acquisition Program Administration (No. UD170034GD).

References

[1] J.F. Lancaster, Phys. Technol. 15 (1984) 73.
[2] H. Dong, W. Hu, Y. Duan, X. Wang, C. Dong, J. Mater. Process. Technol. 212 (2012) 458.
[3] S. Bozzi, A. Helbert-Etter, T. Baudin, B. Criqui, J. Kerbiguet, Mater. Sci. Eng. A 527 (2010) 4505.
[4] P. Liu, Y. Li, H. Geng, J. Wang, Mater. Lett. 61 (2007) 1288.
[5] J. Shang, K. Wang, Q. Zhou, D. Zhang, J. Huang, G. Li, Mater. Des. 34 (2012) 559.
[6] F. Hayat, Mater. Des. 32 (2011) 2476.
[7] C. Xia, Y. Li, U. Puchkov, S. Gerasimov, J. Wang, Vacuum 82 (2008) 799.
[8] P. Xue, B. Xiao, D. Ni, Z. Ma, Mater. Sci. Eng. A 527 (2010) 5723.
[9] P. Xue, D. Ni, D. Wang, B. Xiao, Z. Ma, Mater. Sci. Eng. A 528 (2011) 4683.
[10] J. Feng, X. Songbai, D. Wei, Mater. Des. 42 (2012) 156.
[11] M. Honarpisheh, M. Asemabadi, M. Sedighi, Mater. Des. 37 (2012) 122.
[12] Y. Xiao, H. Ji, M. Li, J. Kim, Mater. Des. 52 (2013) 740.
[13] C. Tan, Z. Jiang, L. Li, Y. Chen, X. Chen, Mater. Des. 51 (2013) 466.
[14] Y. Zhao, D. Li, Y. Zhang, Sci. Technol. Weld. Joining 18 (2013) 354.
[15] P. Carlone, A. Astarita, G.S. Palazzo, V. Paradiso, A. Squillace, Int. J. Adv. Manuf. Technol. 79 (2015) 1109.
[16] T. DebRoy, H. Bhadeshia, Sci. Technol. Weld. Joi. 15 (2010) 266.
[17] A.J. Swiston Jr, T.C. Hufnagel, T.P. Weihs, Scr. Mater. 48 (2003) 1575.
[18] X. Qiu, J. Wang, Sens. Actuators A 141 (2008) 476.
[19] A.H. Kinsey, K. Slusarski, K. Woll, D. Gibbins, T.P. Weihs, J. Mater. Sci. 51 (2016) 5738.
[20] S.H. Kim, M.R. Zachariah, Adv. Mater. 16 (2004) 1821.
[21] S.B. Kim, K.J. Kim, M.H. Cho, J.H. Kim, K.T. Kim, S.H. Kim, ACS Appl. Mater. Interfaces 8 (2016) 9405.
[22] J.H. Kim, M.H. Cho, K.J. Kim, S.H. Kim, Carbon 118 (2017) 268.
[23] K.J. Kim, M.H. Cho, S.H. Kim, Combust. Flame 197 (2018) 319.
[24] V.S. Parimi, S. Huang, X. Zheng, Proc. Combust. Inst. 36 (2017) 2317.
[25] H.-S. Seo, J.-K. Kim, J.-W. Kim, H.-S. Kim, K.-K. Koo, J. Ind. Eng. Chem. 20 (2014) 189.
[26] J.Z. Wen, S. Ringuette, G. Bohlouli-Zanjani, A. Hu, N.H. Nguyen, J. Persic, C.F. Petre, Y.N. Zhou, Nanoscale Res. Lett. 8 (2013) 184.
[27] J.Y. Ahn, J.H. Kim, J.M. Kim, D.W. Lee, J.K. Park, D. Lee, S.H. Kim, Powder Technol. 241 (2013) 67.
[28] M.-S. Shin, J.-K. Kim, J.-W. Kim, C.A.M. Moraes, H.-S. Kim, K.-K. Koo, J. Ind. Eng. Chem. 18 (2012) 1768.
[29] M. Petrantoni, C. Rossi, L. Salvagnac, V. Conédéra, A. Estève, C. Tenailleau, P. Alphonse, Y.J. Chabal, J. Appl. Phys. 108 (2010)084323.
[30] K. Zhang, C. Rossi, P. Alphonse, C. Tenailleau, S. Cayez, J.-Y. Chane-Ching, Appl. Phys. A 94 (2009) 957.
[31] S. Pourmortazavi, S. Hajimirsadeghi, I. Kohsari, M. Fathollahi, S. Hosseini, Fuel 87 (2008) 244.
[32] V.E. Sanders, B.W. Asay, T.J. Foley, B.C. Tappan, A.N. Pacheco, S.F. Son, J. Propul. Power 23 (2007) 707.
[33] A.Y. Dolgoborodov, A. Streletskii, M. Makhov, I. Kolbanev, V. Fortov, Russ. J. Phys. Chem. B 1 (2007) 606.
[34] M.L. Pantoya, J.J. Granier, Propellants Explos. Pyrotech. 30 (2005) 53.
[35] A.Y. Dolgoborodov, A. Streletskii, M. Makhov, V. Teselkin, S.L. Guseinov, P. Storozhenko, V. Fortov, Russ. J. Phys. Chem. B 6 (2012) 523.
[36] A. Plummer, V. Kuznetsov, T. Joyner, J. Shapter, N.H. Voelcker, Small 7 (2011) 3392.
[37] R.J. Jacob, D.L. Ortiz-Montalvo, K.R. Overdeep, T.P. Weihs, M.R. Zachariah, J. Appl. Phys. 121 (2017)054307.
[38] J.J. Granier, M.L. Pantoya, Combust. Flame 138 (2004) 373.